Article:
Grant, ER, Ross, AN orcid.org/0000-0002-8631-3512 and Gardiner, BA (2016) Modelling Canopy Flows over Complex Terrain. Boundary-Layer Meteorology, 161 (3). pp. 417-437. ISSN 0006-8314

https://doi.org/10.1007/s10546-016-0176-3

Boundary Layer Meteorology manuscript No.
(will be inserted by the editor)

Modelling canopy flows over complex terrain

Eleanor R. Grant · Andrew N. Ross · Barry A. Gardiner

Draft: 31st July 2015

Abstract Recent studies of flow over forested hills have been motivated by a number of important applications including understanding CO_2 and other gaseous fluxes over forests in complex terrain, predicting wind damage from trees and modelling wind energy potential at forested sites. Current modelling studies have focused almost exclusively on highly idealised, and usually fully forested, hills. This paper presents model results for a site on the Isle of Arran, Scotland with complex terrain and a heterogeneous forest canopy. The model uses an explicit representation of the

E. R. Grant

Institute for Climate and Atmospheric Science, School of Earth and Environment, Univ. of Leeds, UK.

Present address: British Antarctic Survey, High Cross, Madingley Road, Cambridge, CB3 0ET, UK

A. N. Ross

Institute for Climate and Atmospheric Science, School of Earth and Environment, Univ. of Leeds, UK.

B. A. Gardiner

Forest Research, Northern Research Station, Roslin, Midlothian EH25 9SY, Scotland. Present address: INRA, UMR 1391 ISPA, 33140 Villenave D'Ornon and Bordeaux Sciences Agro, UMR 1391 ISPA, 33170 Gradignan, France.

canopy and a one-and-a-half order turbulence closure for the turbulence within and above the canopy. The validity of the turbulence closure scheme is assessed using the turbulence data from the field experiment before comparing predictions of the full model with the field observations. For near-neutral stability the results compare well with the observations showing that a relatively simple canopy model such as this can accurately reproduce the flow patterns observed with complex terrain and realistic variable forest cover, while at the same time remaining computationally feasible for real case studies. The model allows a closer examination of the flow separation observed over complex forested terrain. Comparison with model simulations using a roughness length parametrization show significant differences, particularly with respect to flow separation and this highlights the need to explicitly model the forest canopy if detailed predictions of the near-surface flow around forests are required.

Keywords Complex terrain, First order mixing length closure, Flow separation, Forest canopy, Numerical modelling

1 Introduction

There has been significant interest over the last few years in modelling the effects of canopy flow over complex terrain. This has been motivated by a number of issues, particularly the need to understand and interpret CO_2 flux measurements over complex forested sites, where advective affects can lead to a significant difference between above-canopy fluxes and the source / sinks within the canopy (Katul et al., 2006; Ross and Harman, 2015). Other important applications include assessing wind damage to trees and estimating potential wind energy resources for wind farms. Realworld sites tend to be complicated, in terms of both the terrain and heterogeneity in the forest canopy. In contrast the vast majority of modelling studies so far have addressed highly idealised problems. Many concentrate on flat, homogeneous canopies (e.g. Pinard and Wilson, 2001). Where they do study heterogeneous problems, these are often highly idealised such as a sharp forest edge (Liu et al., 1996; Yang et al., 2006; Dupont and Brunet, 2008, 2009; Dupont et al., 2011; Banerjee et al., 2013; Schlegel et al., 2015) or idealised fully forested hills (Ross and Vosper, 2005; Ross, 2008; Dupont et al., 2008; Patton and Katul, 2009). The recent paper of Ross and Baker (2013) takes this slightly further by looking at partially forested (but still idealised) hills. There are good reasons for starting with such idealised problems. It allows for a systematic study of the individual processes influencing flow over forest hills. These problems may also be amenable to analytical analysis (e.g. Finnigan and Belcher, 2004). It is also possible to reproduce some of these problems in the laboratory (e.g. Poggi and Katul, 2007) to provide validation data for the models. However, ultimately we need to be able to model flow over real, complex terrain with complicated, heterogeneous forest cover. This study aims to do that. The simulations discussed here are based on the field experiment described in Grant et al. (2015) and the field observations will be used to validate the modelling. The aim is to assess the feasibility of using existing models to tackle such complex problems and to investigate some of the issues faced when making such realistic simulations.

There are currently two principal approaches used for modelling turbulence in canopy flows: mixing length closure schemes (e.g. Pinard and Wilson, 2001; Ross and Vosper, 2005; Banerjee et al., 2013) and large-eddy simulations (LES) (e.g. Brown et al., 2001; Yang et al., 2006; Ross, 2008; Dupont et al., 2008; Patton and Katul, 2009). LES offers advantages in terms of requiring fewer assumptions about the nature of the turbulence in forest canopies, but the excessive computational demands make it usually impractical in terms of modelling realistic cases over large domains, although Schlegel et al. (2015) have demonstrated that this is possible, at least for idealised flow across a forest edge with a real heterogeneous canopy structure. Previous work has shown that while there are limitations in its applicability, mixing length closure schemes actually perform reasonably well in terms of predicting mean flow over relatively flat, homogeneous canopies from both a theoretical (Finnigan and Belcher, 2004) and a practical (Pinard and Wilson, 2001) perspective. In a recent paper Finnigan et al. (2015) have reviewed the applicability and limitations of mixing length closure schemes from a theoretical perspective. In this study we will look at how applicable such schemes are for modelling more complex terrain and heterogeneous forest canopies in reality, using the one-and-a-half order mixing length closure scheme from Ross and Vosper (2005).

In section 2 the model setup is described. Section 3 provides some validation for the mixing length closure by testing the closure assumptions using observational data over complex terrain from Grant et al. (2015). Section 4 presents a comparison of the model and observational results in terms of the mean flow, momentum fluxes and turbulent kinetic energy. The sensitivity of the model to the parametrization of the surface is investigated in Section 5, and the model results are used to better understand the complicated flow separation over a realistic site. Finally section 6 provides some discussion and conclusions.

2 Description of observations and model

The case study used in this paper comes from a field experiment conducted on the Isle of Arran, Scotland during spring 2007. The experiment is described in detail in Grant et al. (2015). The field site is the ridge Leac Gharbh which is situated on the north-east coast of Arran. The ridge is orientated north-west / south-east with the southern end of the ridge being mostly covered with Sitka spruce and mixed deciduous trees. Here we make use of wind speed and direction measurements made from a network of 12 automatic weather stations (AWS) and 3 instrumented towers as described in Grant et al. (2015). The AWS were fitted with cup anemometers and wind vanes at 2m height and were located both within and outside the forest canopy. The 3 towers varied in height from 15 to 23 m with 4 sonic anemometers mounted on each. The towers formed a transect across the forested part of the ridge. The data presented is based on 15-minute average wind speeds and directions. The choice of coordinate system for sonic anemometer measurements in complex, forested terrain is non-trivial, as highlighted by a number of recent studies including Ross and Grant (2015); Oldroyd et al. (2015), however for simplicity and for consistency in comparing with the model, a double rotation into streamwise coordinates is carried out here, as in Grant et al. (2015). This coordinate system means u is the velocity component in the streamwise direction, w is the slope normal velocity component and v is the remaining velocity component in the axis perpendicular to u and w.

Given the uncertainty in the forest parameters and in the upstream flow conditions, and also the local variability in the observations, this study aims to model some generic flow conditions (neutral flow with a $10\,\mathrm{m\,s^{-1}}$ geostrophic wind and different fixed geostrophic wind directions) and compare them with the observational climatology, rather than trying to precisely model particular case studies. The focus here is on near-neutral flow for a couple of reasons. Firstly, much of the previous theoretical work (e.g. Finnigan and Belcher, 2004; Ross and Vosper, 2005; Ross and Baker, 2013) is for neutral flow, and one motivation of the paper is to test how these ideas can be applied to more complex terrain and canopy cover. Secondly, under stable conditions canopy flows are known to decouple, with an in-canopy drainage flow distinct from the above canopy flow (see e.g. Belcher et al., 2012). This is an important problem, but the mixing length closure model described here has not been developed or tested with such flows in mind, and so for this study such regimes are excluded.

Numerical simulations were conducted using the BLASIUS model, originally developed at the UK Met Office and described in Wood and Mason (1993). The model solves the three-dimensional, time-dependent Boussinesq equations of motion in a terrain-following coordinate system. The addition of a canopy drag term and a modified turbulence scheme (see Ross and Vosper, 2005) make it suitable for modelling canopy flows over hills. It has been used for studying a range of idealised problems related to canopy-covered hills (Brown et al., 2001; Ross and Vosper, 2005; Ross, 2008, 2011; Ross and Harman, 2015), partially forested hills (Ross and Baker, 2013) and variable canopy densities (Ross, 2012). The model has been validated against wind tunnel measurements over a hill, and against observations from a flat heterogeneous forest (Ross and Vosper, 2005), but this is the first time the model has been applied to such complex, heterogeneous terrain as this.

The simulations described here use a one-and-a-half order mixing length closure scheme with a prognostic equation for the turbulent kinetic energy, k. The scheme is described in Ross and Vosper (2005), however in summary the eddy viscosity is calculated as $\nu_t = \Gamma_0^{1/2} k^{1/2} l_m$ where Γ_0 is the (assumed constant) ratio between the stress and the energy and l_m is the mixing length, which is constant within the canopy and scales with height above the canopy. In BLASIUS a default value of $\Gamma_0 = 0.357$ is used. The turbulent kinetic energy satisfies

$$\rho \frac{Dk}{Dt} = \rho \nabla \cdot (\nu_t \nabla k) + \tau_{ij} \frac{\partial U_i}{\partial x_j} - \rho \varepsilon \qquad (1)$$

where ρ is the density of the air, U_i is the mean wind speed, τ_{ij} is the Reynolds stress tensor and ε is the dissipation. The Reynolds stress is modelled as $\tau_{ij} \equiv -\rho \overline{u_i' u_j'} = \rho \nu_t S_{ij}$ where $S_{ij} = \partial U_i / \partial x_j + \partial U_j / \partial x_i$ is the deformation tensor. To close the prognostic equation for turbulent kinetic energy requires the dissipation term, ε to be parametrized. This takes the standard form above the canopy ($\varepsilon_{cc} = k^{3/2} \Gamma_0^{3/2} / l_m$), with an enhanced dissipation $\varepsilon_{fd} = Ca|\mathbf{U}|k$ within the canopy (following Wilson et al., 1998) to account for canopy drag rapidly converting energy from large scales to small, quickly dissipated "wake scales". The overall dissipation within the canopy is taken as the maximum of these two terms $\varepsilon = \max(\varepsilon_{cc}, \varepsilon_{fd})$. See also Katul et al. (2004) for a useful discussion of k and $k - \varepsilon$ models applied to canopy flows.

Terrain and land use data (50 m horizontal resolution) came from the Ordnance Survey Landranger and MasterMap products, accessed via EDINA (2011). The model domain was 6 km $\times$ 6 km with 120 grid points in each direction giving a horizontal resolution of 50 m. The domain is centred on the Leac Gharbh ridge. The height of the domain was 5 km with a stretched vertical grid of 80 points giving a vertical res-

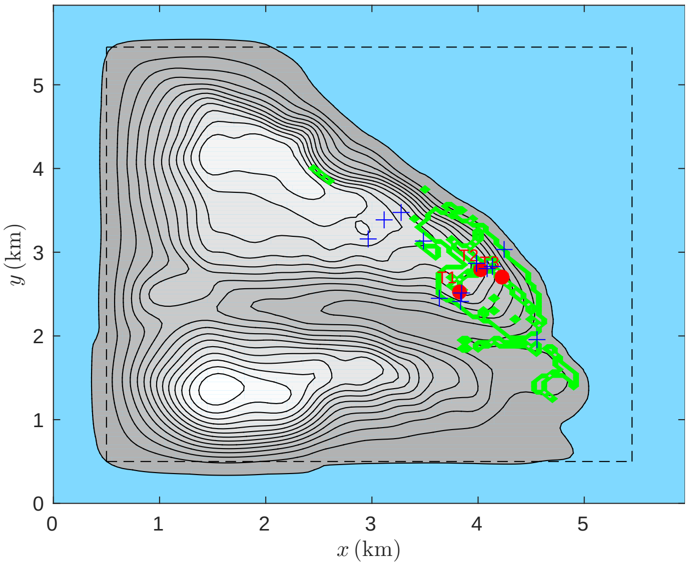

Fig. 1 The model domain used in the BLASIUS simulations. The shaded grey colour denotes the terrain height, with contours every 25m. The solid green line marks the boundary of the forest. The red circles labelled T1-T3 denote the 3 instrument towers and the blue + show the location of the AWS. The light blue area around the edges denotes sea, where a lower roughness length z_0 is used. The dashed line marks the edge of the damping layer.

olution varying from 0.5 m at the surface to approximately 180 m at the top of the domain. In order to keep the model domain to a computationally manageable size lateral periodic boundary conditions were used, with a damping layer applied over the outermost 500m of the domain to relax the solution back towards the geostrophic wind profile. The terrain is also smoothed to zero in the damping layer domain and the surface roughness set to the value over the sea to ensure continuity across the periodic boundaries. Figure 1 shows the model domain and illustrates the topography and forest cover used. The white area around the edges and to the top right is sea.

The location of regions of different land use is accurately obtained from the Ordnance Survey data, however there is significant uncertainty in the correct roughness length and canopy parameters to use in these regions. Field measurements of tree properties made by Forest Research near the field site (Grant et al., 2015) suggest that a canopy height $h = 15\,\mathrm{m}$, uniform canopy density of $0.5\,\mathrm{m}^2\,\mathrm{m}^{-3}$ and canopy drag coefficient $C_d = 0.25$ are broadly representative of the forest cover on the ridge. There is variation in the canopy cover, however given the lack of detailed measurements across the whole ridge and the other uncertainties in the modelling, these representative canopy parameters should be reasonable. The roughness length used over the land outside the forest and at the forest canopy floor is $0.05\,\mathrm{m}$, representative of grassland. Over the sea a lower representative value of $0.005\,\mathrm{m}$ is used. The sensitivity of the results to these roughness lengths will be assessed later. The model simulations were all run to steady state (approx $1000\,\mathrm{s}$ or twice the domain advection time).

3 Validation of mixing length closure

Typically turbulence closure schemes are validated using data from relatively flat, homogeneous sites (e.g. Pinard and Wilson, 2001). To test the validity of the turbulence closure assumptions in BLASIUS over a site with complex, heterogeneous terrain observational data from the field campaign described in Grant et al. (2015) is analysed. The one-and-a-half order turbulence scheme in BLASIUS assumes that the Reynolds stress tensor τ_{ij} is given by $\tau_{ij} = -\rho\overline{u_i'u_j'} = \rho\nu_t S_{ij}$. Even in complex canopy flows scaling analysis suggests that the stress tensor S_{ij} is usually dominated by the vertical gradients of the horizontal velocity components, and so here we focus

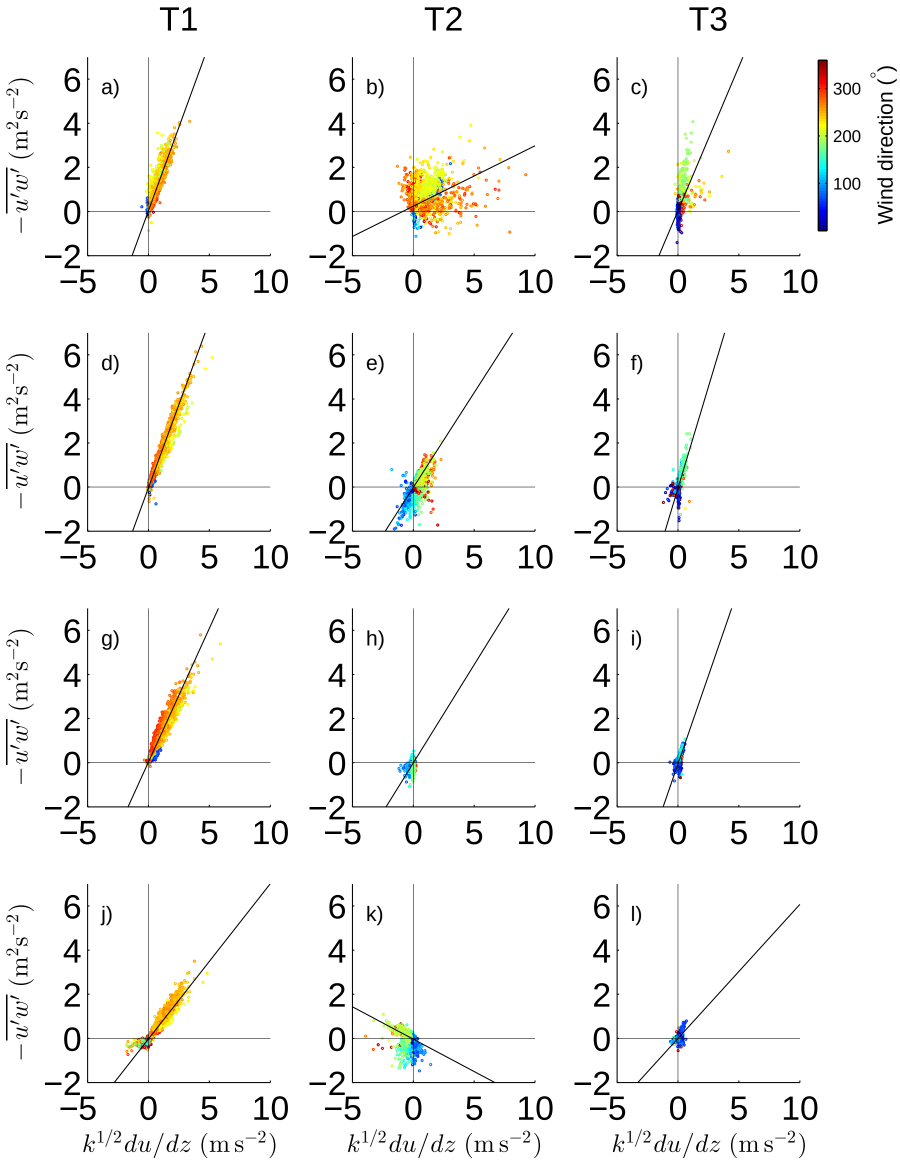

Fig. 2 Momentum flux $\overline{u'w'}$ in streamwise coordinates as a function of $k^{1/2}\partial\overline{u}/\partial z$ where k is the turbulent kinetic energy. The colours denote the direction of the mean wind for each 15-minute averaged data point. The solid line is a best fit line to the data which passes through the origin. The slope of the line is proportional to the mixing length l_m. The three columns correspond to towers T1 (left), T2 (centre) and T3 (right). The rows correspond to the different heights on each tower with the top row corresponding to the top of the tower, and the bottom row the lowest instrument height.

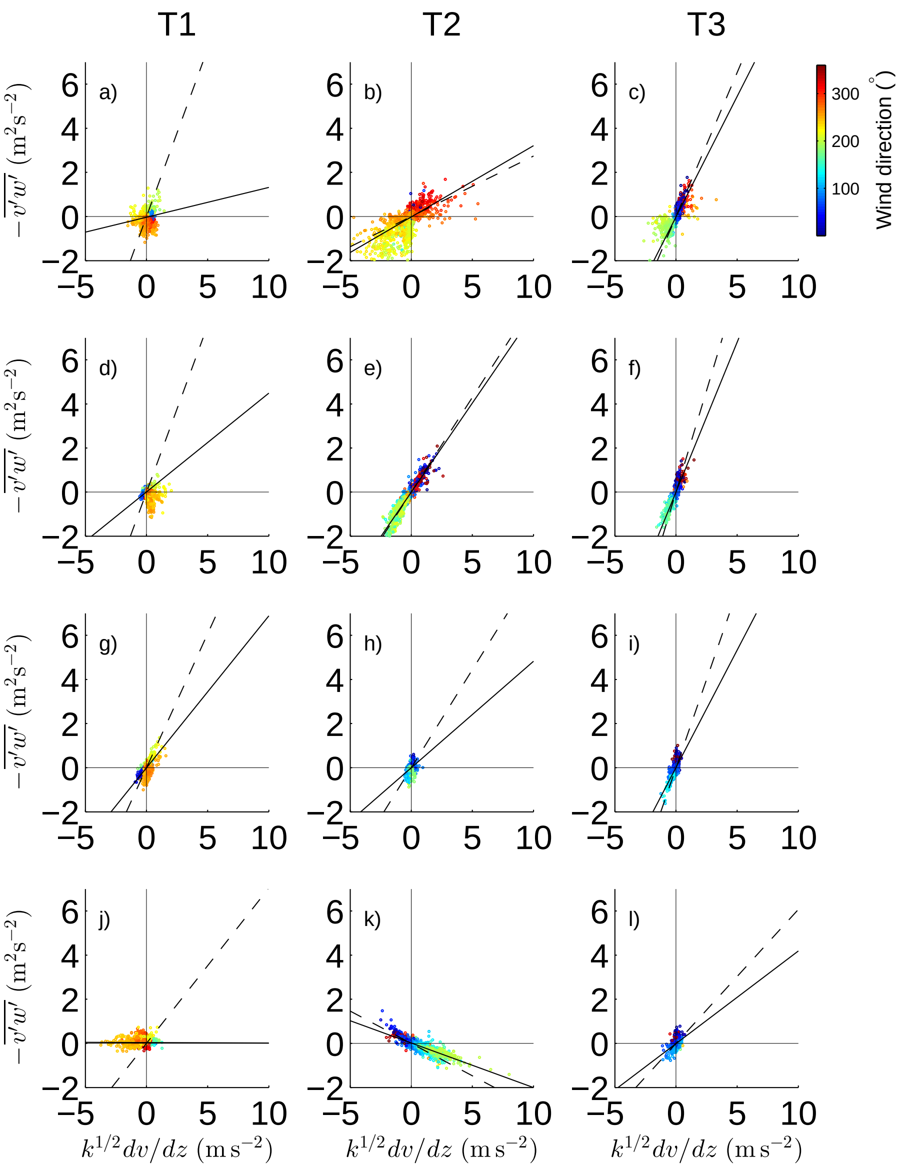

Fig. 3 As for Fig 2, but for $\overline{v'w'}$ as a function of $k^{1/2}\partial\overline{v}/\partial z$. The dotted line shows the slope of the equivalent subplot in Fig 2.

on $-\overline{u'w'} \approx \Gamma_0^{1/2} l_m k^{1/2} \partial u/\partial z$ and $-\overline{v'w'} \approx \Gamma_0^{1/2} l_m k^{1/2} \partial v/\partial z$. The vertical gradients in streamwise coordinate are calculated by first rotating into a fixed frame of reference relative to the ground, calculating the gradients at the midpoints between the observations by finite differencing, linearly interpolating the results back onto the measurement heights and then finally rotating back into the local streamwise coordinates at each height. Here quality controlled data from Grant et al. (2015) for all wind directions and stabilities is used to assess the validity of the closure assumptions. The quality control involves ensuring sufficient data is available in each 15-minute averaging period and also that the data passes the stationarity test of Foken and Wichura (1996) as described in Grant et al. (2015). This quality controlled data amounts to about 4000 data points for T1, 3600 data points for T2 and 2500 data points for T3.

Figure 2 shows the momentum flux, $-\overline{u'w'}$, plotted against $k^{1/2} du/dz$ for the 3 turbulence towers (T1, T2 and T3) situated across the ridge. The linear best fit line through the data is also plotted. The slope of this line is proportional to the average mixing length, l_m with the constant of proportionality being $\Gamma_0^{1/2}$. The results show that for tower T1 the data collapses well, with the mixing length relatively constant with height within the canopy (the best fit line has the same slope at different heights). There is some slight evidence of a decreased mixing length at the lowest height due to the close proximity to the ground. Similar plots of $\overline{v'w'}$ against $k^{1/2} dv/dz$ in Fig. 3 show a relatively small vertical flux of across-stream momentum, suggesting little directional shear and an approximately two-dimensional flow.

In contrast to tower T1, at tower T2, which is surrounded on nearly all sides by trees and where there is often flow separation at the lower two levels, the collapse of the data is far less good. The fluxes are generally lower, and there is significant directional wind shear in the vertical (see Grant et al., 2015, for details). This directional shear is not observed at tower T1 and may be responsible for the poorer data collapse at tower T2. Interestingly there does seem to be a dependence on the mean wind direction, which is most noticeable at the top of T2. For particular wind directions (e.g. easterly winds) the data does seem to collapse, but the slope is a function of the wind direction. For other wind directions (e.g northerly / north-westerly winds) there is no clear collapse. This may suggest that the mixing length is dependent on the flow direction. This would makes sense since it is the upwind forest canopy density which will control the observed mixing length. At the second height down on T2 there is a much stronger linear relationship, but the sign of the flux exhibits a strong dependence on the wind direction. The negative values of $\overline{u'w'}$ are at first glance surprising given the wind speed typically increases with height at this location. Due to the strong direction wind shear however du/dz is actually negative. It is not clear why the data collapse is better at the second height down than at the top of T1, although it might be related to the proximity of the top of the tower to canopy top, or to difficulties in accurately calculating the shear in this region. The strong directional wind shear at the the second height down might also result in a stronger correlation between the local shear and the local turbulent momentum fluxes. A further complication is the presence of a SW-NE aligned fire break across the ridge just to the south of T2 which may impact on the flow for certain wind directions. It is not clear though that the data collapse is worse for cases where the wind is blowing from this direction. At the lowest two measurement heights, in the region of separated flow and where the speeds are lowest, there is little evidence of any linear relationship between $\overline{u'w'}$ and $k^{1/2}d\overline{u}/dz$. At the lowest height, the apparent trend is negative, which is contrary to the underlying assumptions in the closure model and suggests either a non-local source for the turbulent eddies responsible for the momentum transport or errors in the calculation of the wind shear at this location. The scatter however is large and so the relationship is not clear. The plots of $\overline{v'w'}$ against dv/dz show that the cross-stream momentum flux is not insignificant at this site (again, consistent with the importance of directional shear). The first order closure still seems to hold reasonably well, particularly at the second height from the top of the mast. The slopes of the solid and dashed lines are very similar showing that the mixing lengths inferred from $\overline{v'w'}$ are very similar to those derived from $\overline{u'w'}$, which is again encouraging. At the lowest height, as for $\overline{u'w'}$, the data collapses surprisingly well but gives a negative slope. The other noticeable feature at tower T2 is that the sign of the shear term $k^{1/2}dv/dz$ is strongly dependent on wind direction suggesting two different flow regimes for broadly north-easterly and broadly south-westerly flow, which is again consistent with the profiles given in Grant et al. (2015) and with the plots of $k^{1/2}du/dz$.

T3 is taller that T1 and T2, and so the top measurements are above the canopy. Despite this the data collapse is less clear. For much of the time and for certain wind directions the data does lie on a straight line, however again during periods of flow separation there is often a positive value of $\overline{u'w'}$, indicative of the effects of directional shear. The diagnosed mixing lengths are relatively constant with height, similar to those at tower T1. The plots of $\overline{v'w'}$ show a similar collapse of the data to those of $\overline{u'w'}$ and very similar mixing lengths. Values of $\overline{v'w'}$ lie somewhere between those at towers T1 and T2, suggesting that direction shear may be important here, but probably less than at tower T2. The data at the lower heights collapses well, but as for $\overline{u'w'}$ there is a directional dependence on the mixing length at the top of the tower.

Calculating an average mixing length from the slope of the best-fit line using only data with $\overline{u'w'} < 0$ gives fairly consistent results, with mixing lengths in the range of $2.3-3\,$m at most heights on towers T1 and T3, and lower values close to $1.5\,$m at the lowest instrument heights. These mixing length values are surprising consistent with values derived from the plots of $\overline{v'w'}$, particularly at towers T2 and T3 where the directional shear and cross-stream momentum flux are most important. The data from the top of tower T3 remains somewhat different and is separated into two flow regimes. The bulk of the data, for broadly easterly winds with no flow separation, lies on the steeper line with a slope giving $l_m \approx 4.8$ m. This tower is taller than towers T1 and T2 and the instrument is well above the height of the canopy, so one would expect to see an increase in the mixing length at this location under these conditions. The remaining data is predominantly for westerly cases with flow separation and stronger directional shear and is characterised by larger values of the shear term $k^{1/2}du/dz$ but weaker momentum fluxes. Mixing length closure schemes are known to have issues in separated flows (e.g. Ross et al., 2004) and so it is perhaps not surprising that a different behaviour is observed in this separated flow regime.

From all these profiles one can conclude that in many cases (particularly where there is little directional shear) a mixing length closure assumption is reasonable, and that the diagnosed mixing lengths from the observations are consistent with the common assumptions of a constant mixing length in the canopy. Only at T3 do measurements extend much above the canopy, and these seem to suggest a mixing length which increases with height (at least for non-separated flow), although there are not enough measurements to conclude whether this relationship is linear with height as expected from theory. This has important implications for the numerical modelling of canopy flows in complex terrain. There remain a number of cases (particularly at T2 near the summit) where there is flow separation and strong directional shear, and in these cases the mixing length closure assumptions do not appear to hold as well. Some cases with directional shear (e.g. the 2nd height from the top on tower T2) do actually support the assumption of a constant mixing length, and so it may be that it is not the directional shear *per se* which is important, but the fact that the mixing length is strongly dependent on the wind direction due to very different upstream conditions in different directions. For many of the cases where the simple mixing length closure assumptions do not hold the corresponding momentum fluxes are small anyway, and so the overall impact on the mean flow may not be significant. There is also more uncertainty associated with the observations in the cases with significant directional shear. Weak mean flow and larger directional shear make it harder to calculate the gradient terms du/dz in the mean flow in a robust manner. Weak mean winds also lead to more variability in the calculated streamwise coordinate rotations, which may impact on the calculated momentum fluxes. Both of these are likely to increase the scatter in the results as for example is observed in the plots of $\overline{u'w'}$ from the lower two instruments on T2 (Figs. 2(h) and (k)) located deep within the canopy. Overall these results support the use of the one-and-a-half order mixing length closure scheme implemented in the BLASIUS model. The precise impact the regions of directional shear, and the associated errors in the mixing length turbulence closure, have on model predictions of mean flow fields will be investigated in the following section by comparing results from the full model with the observations.

4 Comparison of model and observations

As in Grant et al. (2015), only observational data from near-neutral or transition-to-stable conditions is used in order to allow comparison with the neutral flow model simulations. Two flow regimes of north-easterly and south-westerly are presented here. These are the same cases used in Grant et al. (2015), where a detailed observational analysis of these cases is given. There are some issues with interpreting cup anemometer measurements, particularly in a canopy flow. Firstly, the cup anemometers have a stall speed (notionally $0.7\,\mathrm{m\,s^{-1}}$ in this case) below which they will not turn, and so under low wind conditions (typical in the canopy) they will tend to give an underestimate of the wind speed compared to sonic anemometer measurements. Secondly, at higher wind speeds, the cup will respond both to the mean wind, but also to larger turbulent gusts, and will therefore tend to overestimate the wind speed so the measured wind speed is effectively $\sqrt{U^2+2k}$

Figure 4 shows wind roses from the 12 AWS and 3 tower sites for both observational and model data. The observations are for cases where the wind is broadly north-easterly with the wind direction at AWS ARP (a ridge top site outside the canopy) being between 50° and 90°. This equates to about 15 hours of data. The model results are for a geostrophic wind direction of 90°, which gives a 2m wind direction at AWS ARP of about 80°. Figure 4(a) show wind roses of 15-minute averaged winds from the 15 hours of observational data, while Fig. 4(b) shows the equivalent wind rose plot from the model, with just a single wind value at each location. Note the model is for a representative geostrophic wind speed of $10\,\mathrm{m\,s^{-1}}$. This gives winds at the AWSs which are similar in magnitude to the observations, but the values cannot be directly compared. It is worth noting that the red bins are for mean winds which are close to or below the stall speed of the cup anemometers on the AWS and so the precise values should be treated with some caution. It is likely that these are under-representing the true wind speed due to stalling.

It is however interesting to look at the wind directions and the variations in wind speed across the hill for both the observations and model. In the easterly case there is evidence of flow separation in the observations from a number of the AWS sites (Fig. 4a), with sites within the canopy on the ridge and over the lee slope showing strong deviations from the geostrophic wind. The flow is generally not reversed, but there can be significant variability in wind direction. Outside the canopy there is less variability in wind direction with winds predominantly remaining north-easterly. As might be expected, wind speeds outside the canopy are also higher than those in the canopy. The tower profiles (Fig. 4c) show little sign of separation, with tower T1 (on the lee slope) still showing broadly north-easterly winds, except at the lowest level in the canopy where there is some indication of more south-easterly winds. This appears to be a marginal case of flow separation and highlights how three-dimensional flow separation can be over real terrain, in contrast to previous idealised two-dimensional studies. In this case the model predictions broadly agree with the observations. Outside the canopy the predicted flow is easterly / north-easterly and stronger than inside the canopy (Fig. 4b). Over the upwind slope the flow remains north-easterly, while near the ridge the wind is more along the ridge. The two AWS sites near the forest edge on the lee slope (ARA and ARC) show light winds and complete flow reversal. This is rather more dramatic than the observations, and may reflect the fact that unresolved small scale local features are important in determining wind direction in very light winds and under an adverse pressure gradient. The observations are particularly variable at these sites. The model tower profiles (Fig. 4d) also look very similar to the observations, and even show the same tendency for the flow to become south-easterly at the lowest level on tower T1. The model also shows a similar (though less pronounced) tendency for the wind to turn clockwise at lower levels on tower T2, which is not seen in the observations. This tower is close to the summit of the ridge and so the precise wind direction is likely to be quite sensitive to the exact location of the grid point. In both observations and model, the results at tower T3 on the upwind slope show a north-easterly wind at all levels. Broadly there is agreement between the model and observations in terms of the wind speeds. The highest winds are seen above the canopy, particularly at the top of tower T2 near the ridge summit. The lowest winds in the observations are at the lower levels on towers T1 and T2. The model is slightly different, with low wind speeds low down on tower T1, but slightly higher winds at the bottom of tower T2. Again the differences here perhaps represent the sensitivity of the exact grid location at the ridge top.

Figure 5 is similar to Fig. 4, except that results are for broadly south-westerly winds (observed wind directions in the range 240° to 260° - about 50 hours of data). The model results are for a westerly geostrophic wind (corresponding to a wind di-

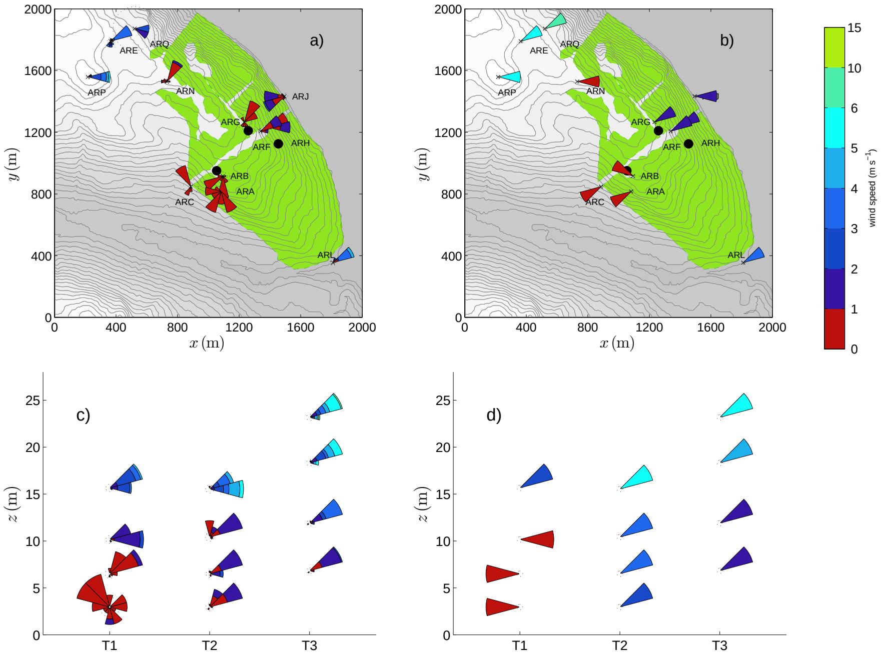

Fig. 4 Wind roses for the 12 AWS sites (a,b) marked with letters ARA to ARQ and 3 tower sites (T1, T2 and T3) (c,d). Results are from observations with north-easterly winds (a,c) and from the model simulation with a $10\,\mathrm{m\,s^{-1}}$ easterly geostrophic wind (b,d). The grey shading is height, with contours plotted every 10m. On the maps the locations of the three towers are marked with black circles.

rection of about 260° at 2m at AWS ARP). The ridge is asymmetric with the eastern slope steeper than the western slope and so for westerly winds the lee slope is steeper and flow separation occurs more easily than for easterly winds. The AWS observations (Fig. 5a) show very weak winds and reversed flow at all the AWS sites near the ridge and over the lee slope (ARF, ARG, ARH, ARN). Even the AWS on the coast (ARJ) outside the forest shows reversed flow. The observations show large deviations in the flow near the upwind canopy edge as well (ARA, ARB, ARC), possible due to canopy edge effects or local features of the terrain or canopy. The tower observations

(Fig. 5c) corroborate this picture. Tower T3 over the lee slope shows reversed flow up to the top (about 23 m), which is well above canopy top. Tower T2 appears to be close to the separation point and the lowest two instrument heights show reversed flow, the flow is roughly southerly at the next height, and the flow is still westerly at the top of the tower. Again the model shows very similar behaviour to the observations (Fig. 5c), with the AWS sites over the lee slope demonstrating reversed flow. The directions are similar to those seen in the observations. The most noticeable difference is that the model shows more consistently westerly winds over the upwind slope compared to the observations (ARA, ARB, ARC). Since these sites also showed more variability in the observations in the easterly wind cases it seems likely that the deviations are due to unresolved local features of the terrain or forest canopy. The model profiles from the tower sites (Fig. 5d) show a remarkable similarity to the observations, capturing the flow reversal at tower T3 and the turning of the wind with height at tower T2. The magnitudes of the model winds also appear to vary between locations in a similar way to the observations. As a sensitivity test to the choice of geostrophic wind speed in the model an additional simulation for the south-westerly case was done with a higher geostrophic wind speed of $20\,\mathrm{m\,s^{-1}}$. Results for the sensitivity test (not shown) were very similar to Fig. 5. Visually, there were only very minor differences in the normalised profiles, most noticeably at T2. This supports the comparison of the model with normalised observations over a range of background wind speeds. It also highlights the sensitivity of T2, which is perhaps not surprising given its proximity to the separation point.

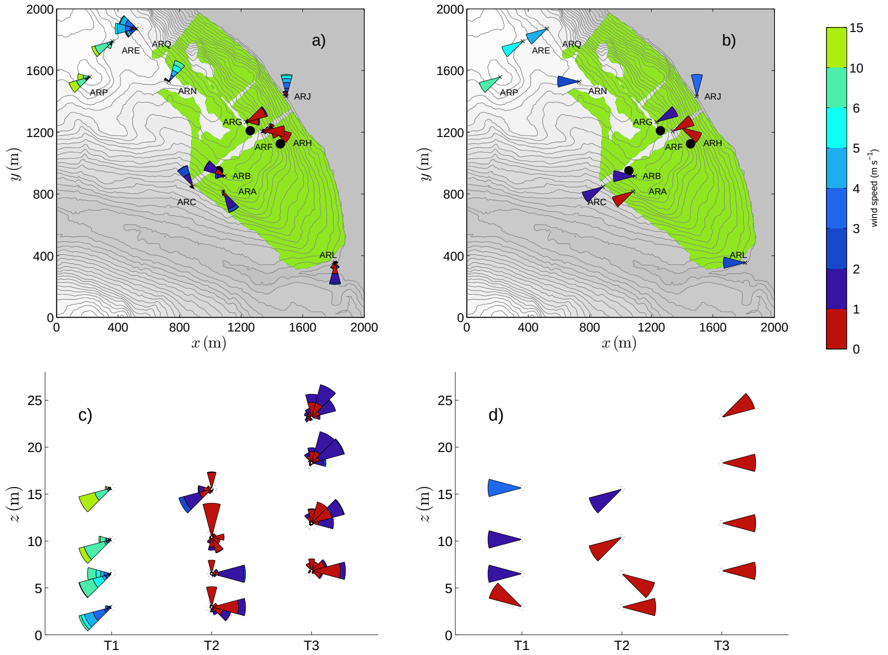

Fig. 5 Wind roses for the 12 AWS sites (a,b) marked with letters ARA to ARQ and 3 tower sites (T1, T2 and T3) (c,d). Results are from observations with south-westerly winds (a,c) and from the model simulation with a $10\,\mathrm{m\,s^{-1}}$ westerly geostrophic wind (b,d). The grey shading is height, with contours plotted every 10m. On the maps the locations of the three towers are marked with black circles.

Figures 6 and 7 provide a more detailed comparison of the mean wind profiles from the three towers, and also the profiles of momentum fluxes and turbulent kinetic energy. To allow for a more quantitative comparison between observations and model the profiles are all normalised using a reference velocity U_{ref} which, for both the observations and the model, is taken as the wind speed at the height of the highest instrument on the upwind tower (tower T1 for south-westerlies and tower T3 for north-easterlies). This normalisation is to account for differences in the background windspeed between the model and the different observations. Table 1 gives the value

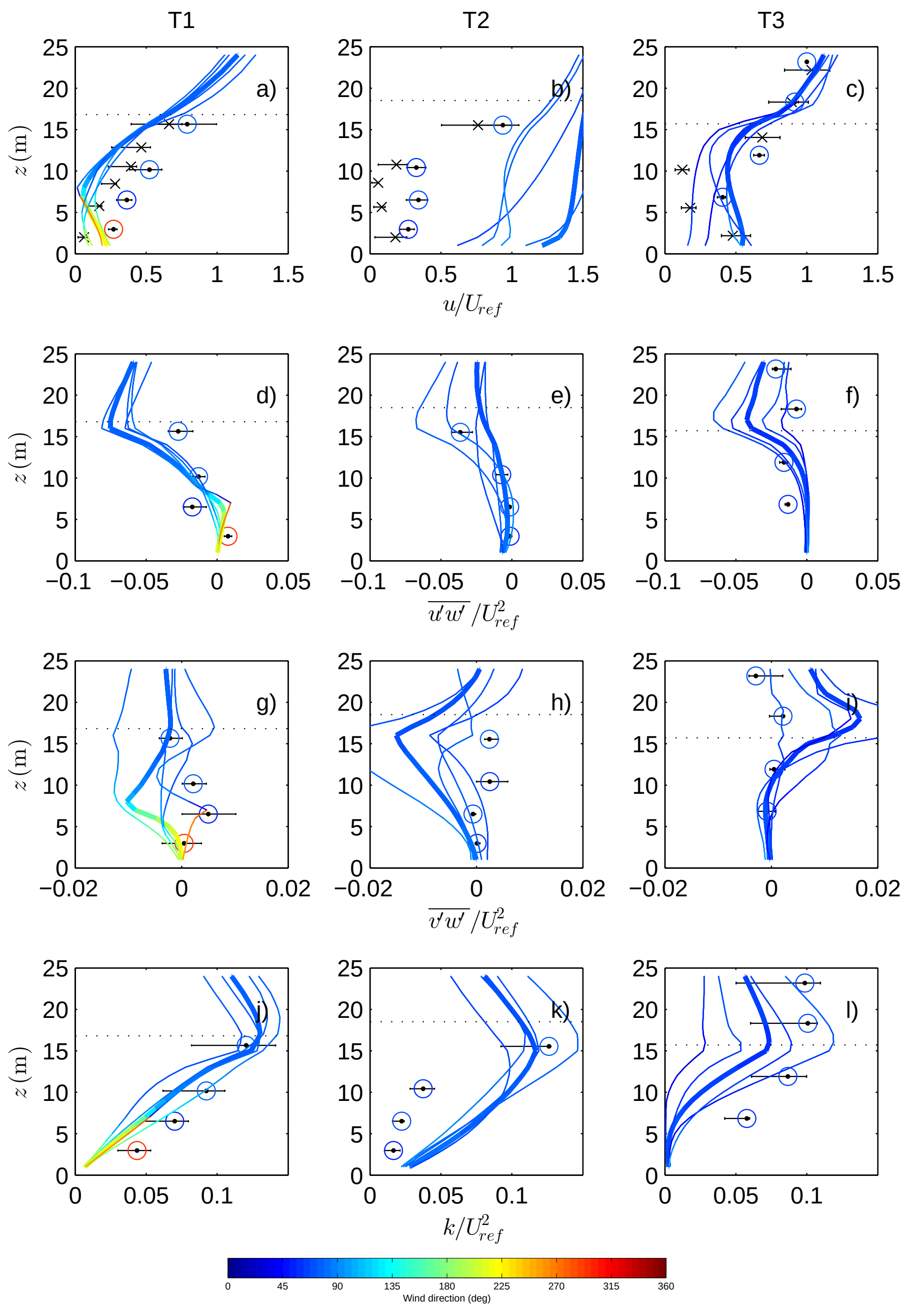

Fig. 6 Profiles for the north-easterly case of (a-c) wind speed, (d-f) streamwise momentum flux $\overline{u'w'}$, (g-i) across-stream momentum flux $\overline{v'w'}$ and (j-l) turbulent kinetic energy, all normalised with a reference velocity U_{ref} taken at the height of the top instrument on the upstream tower T3. Symbols show the mean value from the observations and the error bar shows the interquartile range. The coloured circles represent measurements from the sonic anemometers, with the colour denoting the wind direction. The crosses are measurements from the cup anemometers on the towers. The solid lines show interpolated model profiles at the site of the tower (thick line) and at points 25m to the north, south, east and west of the tower (thin lines), again coloured according to wind direction. The horizontal dotted line marks the approximate canopy top at each tower.

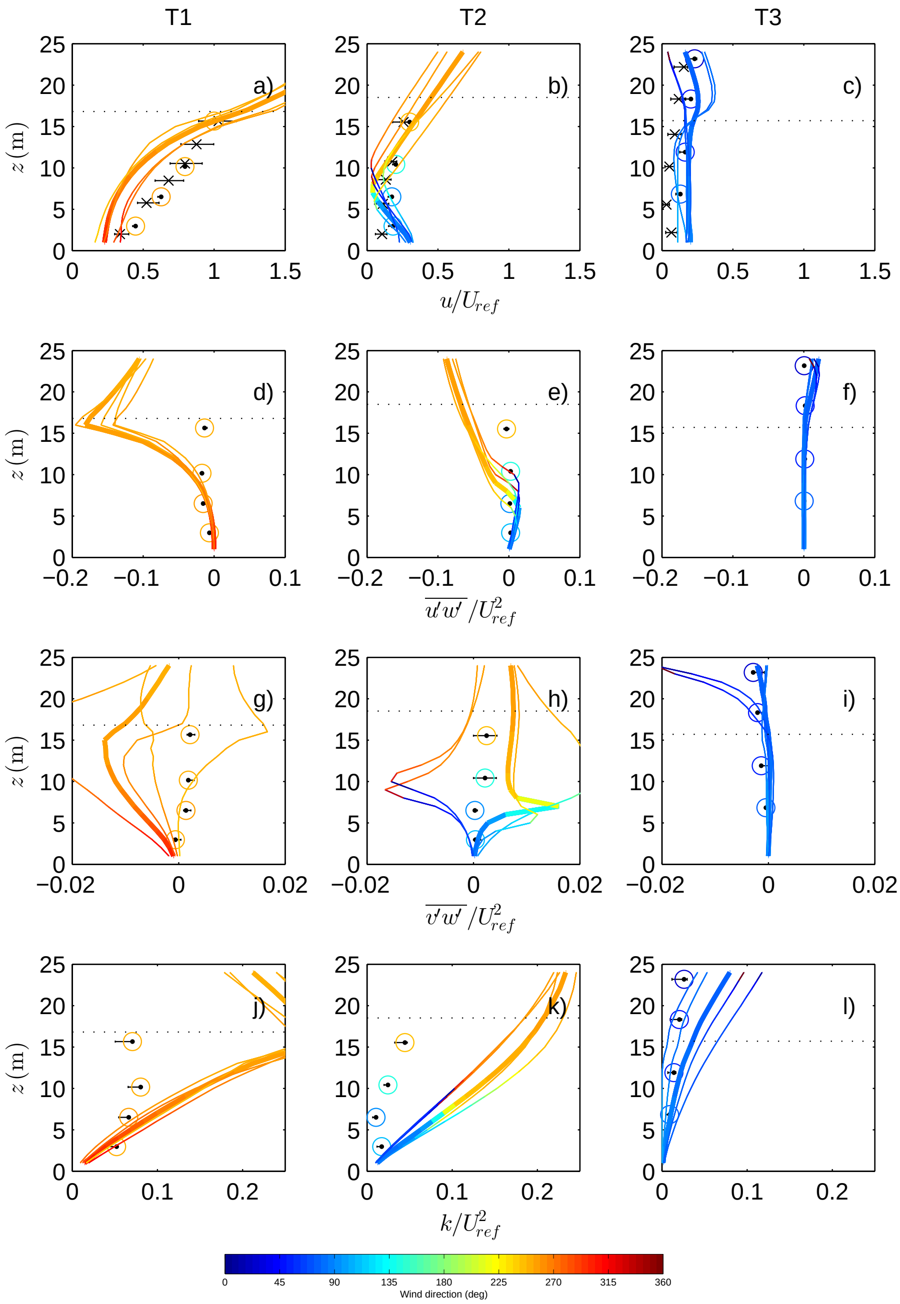

Fig. 7 As for Fig 6, but for the south-westerly case with U_{ref} taken as the top of tower T1.

Table 1 Values of the reference wind speed U_{ref} from the observations (median and interquartile range) and from the model for the north-easterly and south-westerly cases.

Wind direction	Reference tower	Median wind ($\mathrm{m\,s^{-1}}$)	Interquartile range ($\mathrm{m\,s^{-1}}$)	Model wind ($\mathrm{m\,s^{-1}}$)
NE	T3	4.3	2.8 – 5.9	5.4
SW	T1	10.0	7.9 – 12.5	3.7

for U_{ref} from the model and the median and interquartile range from the observations for each wind direction. Several interpolated model profiles are shown, one from the location of each tower and 4 more from 25 m north, south, east and west of the tower (25 m is half the grid resolution of the model) to give an idea of the spatial variability in the model, and hence the possible uncertainty in the model-observation comparison. It is worth noting that the mean wind speeds measured by the cup anemometers are lower than those measured by the sonic anemometers as a result of stalling at low wind speeds in the canopy. This problem is particularly noticeable in Fig 6(a)-(c) due to the lower wind speeds in the north-easterly flow conditions.

For north-easterly cases (Fig 6) the model mean wind profiles at towers T1 and T3 are in reasonable agreement with the observations, however the modelled profiles at tower T2 appear to significantly overpredict the wind speed, although they do capture a profile with fairly constant wind speeds in the canopy and increasing wind speeds above. There is also a large spread between the different model profiles suggesting a region of complex canopy cover with large differences in wind speed over short spatial distances. Bearing this is mind, along with the relatively simple treatment of the canopy properties (uniform canopy height and density everywhere within the canopy) it is perhaps not surprising that the model and observations show some discrepancy. Tower T2 is characterised by quite different canopy cover to the east (relatively sparse larch) and to the west (dense spruce), and there is a fire break to the south, so the uniform canopy parameters are not necessarily a good approximation at this location. Interestingly the profiles of streamwise momentum flux, $\overline{u'w'}$, are in good agreement at all three towers. Note also that there is very little variability in the normalised observations of streamwise momentum flux, suggesting that the single reference velocity at the top of tower T3 provides a good scaling for the momentum flux. The relative accuracy of the streamwise momentum flux predictions at T2 is likely to be due to the fact the model captures the right wind shear profile throughout most of the canopy, it's just that the wind speeds are consistently too large. In contrast the profiles of $\overline{v'w'}$ show generally less good agreement between model and observations. The model profiles do demonstrate a significant degree of variability suggesting that $\overline{v'w'}$ is sensitive to the details of the local canopy and flow structure. Comparisons of turbulent kinetic energy profiles between the model and observations are also reasonable at T1 and T3, although at T2 the model appears to consistently overpredict the turbulent kinetic energy within the canopy, which may be related to the overprediction of the wind speeds in this case.

For south-westerly cases (Fig 7) the model mean wind profiles at T2 and T3 show reasonable agreement with the observations, although the model seems to predict more wind shear at T2 than is seen in the observations. At T1, the comparison is a little less good, with the model underpredicting wind speeds below canopy top and too strong a shear near canopy top. T1 is sat on a small outcrop, and in south-westerly winds the flow is likely to accelerate over this outcrop, rather than passing through the upwind canopy, but this feature is not well resolved by the model with the given 50m horizontal resolution. Streamwise momentum fluxes are also in reasonable agreement at most locations, except at the top of towers T1 and T2 where the model predicts a much more rapid increase in the momentum flux than was observed. There is slightly more wind shear in the model wind profiles, but not enough to account for the large increase in momentum flux. The model profiles are very consistent and so this does not appear to be due to spatial heterogeneity. It may be due to slight differences in the canopy height between the model and observations, since the model assumes a constant height of 15 m, or due to vertical variations in the canopy structure which are not represented in the model simulation. Once again across-stream momentum fluxes $\overline{v'w'}$ are very variable and show little agreement between model and observations except at T3. This highlights the very three-dimensional nature of the flow at T1 and T2. For the south westerly cases turbulent kinetic energy profiles seem to be overpredicted by the model at most heights, even where the momentum fluxes are in reasonable agreement. This is most pronounced at T1 and T2. The overprediction of shear near the canopy top may lead to extra generation of turbulent kinetic energy in the model, which is then mixed down into the canopy. A further possibility is that the simple representation of dissipation used in the model is not correct in complex heterogeneous canopies. Further work is needed to understand these discrepancies.

Overall the model reproduces surprisingly well the observed patterns of wind speed and direction over the hill. Those sites where the agreement is less good appear to be primarily located close to the forest edge or near the ridge top at tower T2.

The model also appears to often capture the observed streamwise momentum fluxes, although the across-stream momentum fluxes and turbulent kinetic energy profiles are not always captured as accurately. The agreement gives confidence in using the model results to study more closely the patterns of mean flow and flow separation over the ridge.

5 Flow separation and sensitivity to surface parametrization

The results of Ross and Vosper (2005) suggested that flow separation is an intrinsic feature of uniform canopy flows over idealised hills, and that this is fundamentally different to flow separation over a hill with a rough surface. Here the sensitivity of the model results to the surface parametrization over a more complex and realistic hill is investigated, with particular focus on flow separation.

To test the importance of explicitly resolving the canopy in these simulations the westerly wind case was re-run with the forest canopy being represented by a roughness length parametrization rather than with the explicit canopy model. The roughness length was chosen to match the equivalent roughness of the canopy, $z_0 = 0.35$ (see e.g. Ross and Vosper, 2005). All other aspects of the simulation were unchanged. Figure 8 shows the wind roses from this simulation. In comparison with Fig. 5 there is clearly less strong flow separation with the roughness length parametrization of the surface. The sites that would be in the canopy over the lee slope show a flow which is slowed and deflected along the slope to the south rather than being completely reversed as occurs with the canopy model. Outside the canopy there is little difference between the results, suggesting that the impact of the canopy is relatively localised. In

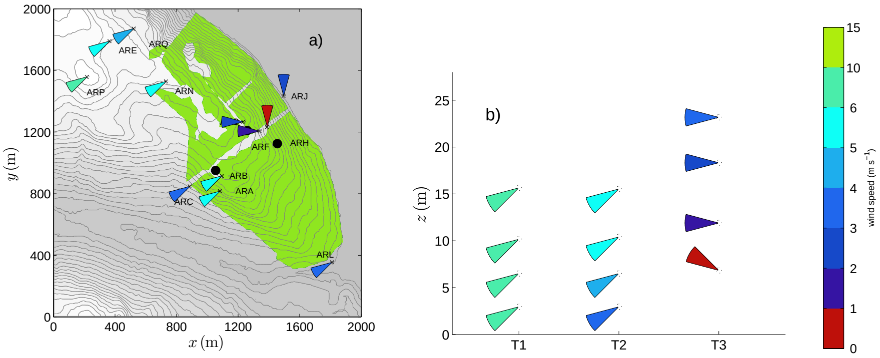

Fig. 8 Wind roses from the model simulation with westerly winds and a roughness length parametrization of the canopy. Results are shown at the 12 AWS sites (a) and the 3 towers (b).

the vertical (not shown) the region in which the flow is reversed or strongly deflected appears to extend up to about 55m above ground level (40m above the canopy top) with the explicit canopy model. In contrast, with the roughness length parametrization the depth and horizontal extent of the region of strongly deflected flow is much reduced, reaching a maximum height of only about 12m above ground level. This suggests that even above the canopy, perhaps up to a couple of times the canopy height, the flow may be fundamentally different under conditions of flow separation depending on the way the effect of the canopy is modelled.

In three dimensions it is hard to identify flow separation in the velocity field. Unlike in two dimensions it is not simply a matter of looking for reversed flow since the flow may be deflected rather than reversed. This makes interpreting the flow pattern based on point observations tricky. Using the model allows a better understanding of the flow across the whole ridge, but it is still difficult to identify flow separation from near surface winds. As Hunt et al. (1978) showed, flow separation is associated with a singularity in the surface stress field and this can provide an alternative method for identifying points or lines where the flow separates from or reattaches to the surface in three-dimensional flows. The surface stress is given by $\partial\mathbf{u_s}/\partial n$ where $\mathbf{u_s}$ is the velocity tangential to the surface and n is the normal to the surface and so the surface stress gives an indication of the flow direction at the surface, but has the advantage of being non-zero, except where flow separates or reattaches. Wood (1995) suggested using plots of surface stress "streamlines" or streaks to identify these singularities. The streaks are plotted by calculating a series of two-dimensional surface trajectories (x,y), where the two horizontal components of the surface stress take the role of the velocity field so

$$\frac{dx}{dt} = \tau_x \quad \frac{dy}{dt} = \tau_y. \tag{2}$$

The streaks are initialised from a series of points across the model domain and then calculated by integrating the trajectories forward and backwards for a specified length time. This works well for the examples used by Wood (1995), however the large difference between surface stress values inside and outside the canopy means that streaks in the canopy are very short. To circumvent this problem, we use a longer integration time, but limit the length of the streaks plotted so that streaks outside the canopy are not too long. The surface stresses are interpolated from the model grid using bilinear interpolation and the integration is carried out using the ode45 function in Matlab. Using this approach and integrating forward numerically from $t = 0$ to $t = 20000$, and limiting the length of the streaks to 500 m gives much more even lengths of streaks inside and outside the canopy, and makes visualisation of flow separation much easier in partially forested flows. Locations where the surface stress streaks all converge at a line or point are associated with flow separating from the surface, while locations where the surface stress streaks all diverge from a line or point are associated with flow reattaching to the surface.

Figure 9 shows plots of the surface stress streaks calculated from the model. Forward trajectories (blue) show flow separation and backward trajectories (red) show reattachment. Wind direction vectors are also plotted at the points where trajectories are initiated. For the easterly wind simulation (Fig. 9a) the surface stress plot clearly illustrates the flow separation occurring over the lee slope on the forested part of the ridge. There is one clear separation line just upwind of the ridge summit stretching right along the forested part of the ridge there is also some indication of a second separation line downwind of the ridge on the southern shoulder of the ridge. Reattachment appears to occur at a singular point on the lee slope close to $x = 1300\,\mathrm{m}$ and $y = 1100\,\mathrm{m}$. This highlights the rather complicated three-dimensional structure of the flow separation over a real ridge with heterogeneous canopy cover in comparison with previous idealised two-dimensional modelling and laboratory studies. To the north where there is no forest cover then the stress streaks pass right over the ridge showing that flow separation does not occur, even though the ridge is slightly higher at this point. Around the southern edge of the ridge, outside the canopy the stress streaks run more or less parallel to the lower edge of the canopy and the contours. This demonstrates the importance of flow around the southern end of the ridge in easterly flow.

In contrast, for the westerly case (Fig. 9b) where the steep eastern slope of the ridge is on the downwind side there is clear evidence of flow separation all along the summit of the ridge, with reattachment occurring somewhere off the coast. Even without the forest canopy this slope is steep enough to generate flow separation. In this case there is a single separation line running right down the ridge. Outside the canopy the separation line is downwind of the ridge summit, while within the canopy separation occurs nearer the ridge summit. The flow off the coast remains almost parallel to the ridge and to the coastline, suggesting that the region of separated flow extends well beyond the foot of the ridge and is therefore much larger than in the easterly wind case. The streaks in this case also suggest a rather less important role for flow around the southern end of the ridge in westerly flow. These figures support the interpretation of the flow separation based on the observed and model wind fields made above and highlight the differences between cases with steep lee slopes where flow separation would occur anyway (westerly flow) and less steep lee slopes, where flow separation requires the presence of the canopy (easterly flow).

The conclusions on the sensitivity of the results to the explicit canopy parametrization are supported by the surface stress plot for the roughness length simulations. For the easterly wind case (Fig. 9c) no flow separation was observed at all in the surface stress streaks with a roughness length parametrization, in clear contrast to the simulation with an explicit canopy. For the westerly case (Fig. 9d) a clear separation line downwind of the summit of the ridge is apparent with the roughness length parametrization. Outside the canopy the streaks look very similar in the two simulations. Inside the canopy, parametrizing the canopy by a roughness length shifts the flow separation further down the lee slope, and significantly reduces the variability caused by the heterogeneous canopy cover and channelling through gaps in the canopy. Explicitly modelling the canopy appears to be essential to capture the flow

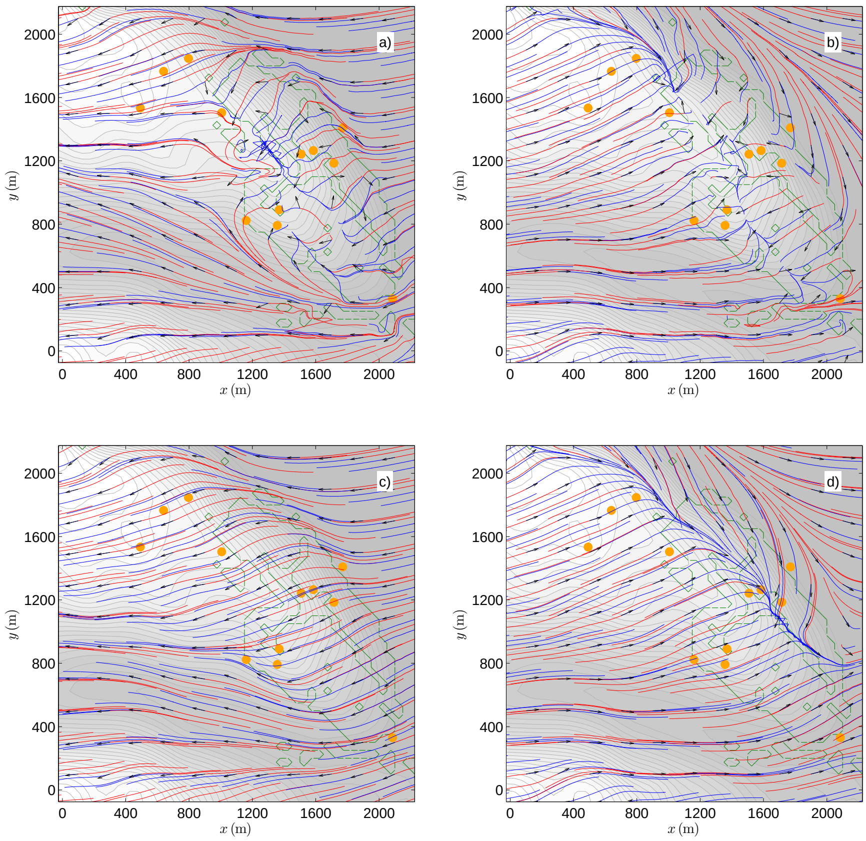

Fig. 9 Surface stress streaks from the model (forward trajectories - blue lines, backward trajectories - red lines) plotted over the height contours (at 10m intervals). Also plotted are wind direction arrows. Results are shown for easterly (a, c) and westerly (b, d) winds. Subfigures a), b) are with the explicit canopy model and c), d) are with a roughness length parametrization of the canopy. The orange dots show the sites of the AWS.

separation in the easterly case with a shallow lee slope, and even in the westerly case with a steeper lee slope the explicit canopy model significantly changes the location and magnitude of the separated region.

6 Discussion and conclusions

Flow over realistic complex terrain with variable forest cover, such as the Leac Gharbh ridge, is complicated and the local wind direction depends strongly on the local terrain and forest cover. Burns et al. (2011), one of the few other observational studies in complex terrain, draws similar conclusions. For flow which is close to neutral, high resolution numerical simulations with an explicit canopy model reproduce many of the features of the observed flow, however high quality input data sets for the terrain and the forest canopy are essential. High resolution terrain data sets are generally available, however details of forest canopy parameters are generally harder to obtain and require dedicated surveys. Available mapping products may provide details of the forest coverage, but they rarely contain details on the nature of the forest, the canopy height, or the canopy density. These details are essential for successful modelling of the flow in or near the canopy. Other recent studies (Burns et al., 2011; Desmond et al., 2014; Schlegel et al., 2015) have also highlighted the need for detailed canopy structure to accurately model heterogeneous canopy flows. Indeed in their study Desmond et al. (2014) saw more sensitivity to realistic canopy structure (particularly vertical structure) than they did to the turbulence closure model used. Recent progress using lidar offers exciting possibilities for detailed three-dimensional mapping of canopy structure (Boudreault et al., 2015), but unfortunately such a survey was not available at this site.

Near the edge of the forest canopy there appears to be greater discrepancy between the model and observations. This is partly due to the limitations of the forestry data, but more fundamentally may be linked to the horizontal resolution of the simulations. At the edge of a uniform canopy the flow adjusts to the canopy over a distance of order $6L_c$ where $L_c = 1/(C_d a)$ is the canopy adjustment length scale (Belcher et al., 2012; Ross and Baker, 2013). For the canopy parameters here this gives $L_c = 4$ m and so the flow adjusts over a distance of about 24 m, roughly half of the horizontal grid spacing. Therefore the details of flow near the canopy edge will not be captured accurately. Unfortunately this is often likely to be the case in real simulations where the desired horizontal resolution has to be balanced with the overall computational requirements of the simulation. The idealised simulations of Ross and Baker (2013) suggest that at a distance greater than about $6L_c$ from the canopy edge the flow in the canopy is dominated by the effect of the hill and not the canopy edge. This also seems to be the case in these more realistic simulations with complex terrain and forest cover since the agreement between observations and model at sites away from forest edges is much better. A further complication is that adjustment can take much longer for non-uniform canopies with a sparse sub-canopy trunk space (Dupont et al., 2011) due to sub-canopy jets penetrating deep into the forest, although the dense canopy cover over most of this field site makes this relatively unlikely.

The other significant discrepancy appears to be at tower T2, particularly in easterly wind cases. It may be that this site, near the ridge top and close to the line of separation is particularly sensitive to small changes in the measurement position. This location is also where the assumptions of a mixing length turbulence closure seemed to be weakest, with a less clear relationship between the momentum flux and the observed shear stress and with a strong directional shear. It is possible that these factors are linked and that part of the reason for the slightly larger disagreement between model and observations near the ridge top is the limitations of the model turbulence closure scheme at this point. More work, possibly using computationally expensive higher resolution simulations with the current turbulence closure scheme or large-eddy simulations, is likely to be required to identify the real cause of this discrepancy.

Although there is some debate in the literature about the suitability of mixing-length closure schemes for canopy flows, these results suggest that such a model does reproduce the main features of the mean flow seen in these observations over complex terrain, at least in near-neutral flow. In part this may be due to the fact that advection is important in the canopy and that this is driven by pressure gradients which are to leading order a result of inviscid flow (see for example the analytical model of Finnigan and Belcher, 2004, for flow over a forested hill). Using the model results allows a far more detailed understanding of the flow separation over such a complicated site than is possible with the observations alone. The role of the canopy in promoting flow separation over gentler slopes, and of shifting the location of flow separation nearer the ridge over steeper slopes, seems clear and is in accord with theoretical ideas developed by Finnigan and Belcher (2004) and Ross and Vosper (2005) over idealised two-dimensional ridges. In contrast, simulations with a roughness length parametrization fail to correctly predict the flow separation and pressure field over the hill. While simulations such as this require a high vertical and horizontal resolution in order to correctly represent the canopy, the simplicity of the one-and-a-half order closure scheme does mean that this approach is at least feasible for realistic high resolution simulations of flow within and above forest canopies. In contrast, more complicated approaches such as large-eddy simulations are at present usually computationally unfeasible for modelling realistic flows with complex topography and forest cover. Of course, for real applications stability effects are also important, particularly in night time drainage flow conditions, and further work needs to be done to see how well mixing-length schemes such as that used here can perform in these cases.

Acknowledgements This work was funded by the Natural Environmental Research Council (NERC) grant NE/C003691/1. ERG would like to acknowledge additional support through a NERC Collaborative Award in Science and Engineering (CASE) award with Forest Research.

References

Banerjee T, Katul G, Fontan S, Poggi D, Kumar M (2013) Mean flow near edges and within cavities situated inside dense cavities. Boundary-Layer Meteorol 149:19–41, DOI 10.1007/s10546-013-9826-x

Belcher SE, Harman IN, Finnigan JJ (2012) The wind in the willows: Flows in forest canopies in complex terrain. Annu Rev Fluid Mech 44:479–504, DOI 10.1146/annurev-fluid-120710-101036

Boudreault LE, Bechmann A, Tarvainen L, Klemedtsson L, Shendryk I, Dellwik E (2015) A LiDAR method of canopy structure retrieval for wind modeling of heterogeneous forests. Agric For Meteorol 201:86–97, DOI 10.1016/j.agrformet.2014.10.014

Brown AR, Hobson JM, Wood N (2001) Large-eddy simulation of neutral turbulent flow over rough sinusoidal ridges. Boundary-Layer Meteorol 98:411–441, DOI

10.1023/A:1018703209408

Burns SP, Sun J, Lenschow DH, Oncley SP, Stephens BB, Yi C, Anderson DE, Hu J, Monson RK (2011) Atmospheric stability effects on wind fields and scalar mixing within and just above a subalpine forest in sloping terrain. Boundary-Layer Meteorol 138:231–262, DOI 10.1007/s10546-010-9560-6

Desmond CJ, Watson SJ, Aubrun S, Avila S, Hancock P, Sayer A (2014) A study on the inclusion of forest canopy morphology data in numerical simulations for the purpose of wind resource assessment. J Wind Eng Ind Aerodyn 126:24–37, DOI 10.1016/j.jweia.2013.12.011

Dupont S, Brunet Y (2008) Edge flow and canopy structure: A large-eddy simulation study. Boundary-Layer Meteorol 126:51–71, DOI 10.1007/s10546-007-9216-3

Dupont S, Brunet Y (2009) Coherent structures in canopy edge flow: a large-eddy simulation study. J Fluid Mech 630:93–128, DOI 10.1017/S0022112009006739

Dupont S, Brunet Y, Finnigan JJ (2008) Large-eddy simulation of turbulent flow over a forested hill: Validation and coherent structure identification. Quart J Roy Meteorol Soc 134:1911–1929, DOI 10.1002/qj.328

Dupont S, Bonnefond JM, Irvine MR, Lamaud E, Brunet Y (2011) Long-distanec edge effects in a pine forest with a deep and sparse trunk space: In situ and numerical experiments. Agric For Meteorol 151:328–344, DOI 10.1016/j.agrformet.2010.11.007

EDINA (2011) Digimap Ordnance Survey service. URL http://edina.ac.uk/digimap

Finnigan JJ, Belcher SE (2004) Flow over a hill covered with a plant canopy. Quart J Roy Meteorol Soc 130:1–29, DOI 10.1256/qj.02.177

Finnigan JJ, Harman IN, Ross AN, Belcher SE (2015) First order turbulence closure for modelling complex canopy flows. Quart J Roy Meteorol Soc 141:2907–2916, DOI 10.1002/qj.2577

Foken T, Wichura B (1996) Tools for quality assessment of surface-based flux measurements. Agric For Meteorol 78:83–105, DOI 10.1016/0168-1923(95)02248-1

Grant ER, Ross AN, Gardiner BA, Mobbs SD (2015) Field observations of canopy flow over complex terrain. Boundary-Layer Meteorol 156:231–251, DOI 10.1007/s10546-015-0015-y

Hunt JCR, Abell CJ, Peterka JA, Woo H (1978) Kinematical studies of flow around free or surface mounted obstacles; applying topology to flow visualisation. J Fluid Mech 86:179–200, DOI 10.1017/S0022112078001068

Katul GG, Mahrt L, Poggi D, Sanz C (2004) One- and two-equation models for canopy turbulence. Boundary-Layer Meteorol 113:81–109, DOI 10.1023/B:BOUN.0000037333.48760.e5

Katul GG, Finnigan JJ, Poggi D, Leuning R, Belcher SE (2006) The influence of hilly terrain on canopy-atmosphere carbon dioxide exchange. Boundary-Layer Meteorol 118:189–216, DOI 10.1007/s10546-005-6436-2

Liu J, Chen JM, Black TA, Novak MD (1996) $e-\varepsilon$ modelling of turbulent air flow downwind of a model forest edge. Boundary-Layer Meteorol 77:21–44, DOI 10.1007/BF00121857

Oldroyd HJ, Pardyjak ER, Huwald H, Parlange MB (2015) Adapting tilt corrections and the governing flow equations for steep, fully three-dimensional, mountainous terrain. Boundary-Layer Meteorol Online First:1–27, DOI 10.1007/s10546-015-

0066-0

Patton EG, Katul GG (2009) Turbulent pressure and velocity perturbations induced by gentle hills covered with sparse and dense canopies. Boundary-Layer Meteorol 133:189–217, DOI 10.1007/s10546-009-9427-x

Pinard JDJP, Wilson JD (2001) First- and second-order closure models for wind in a plant canopy. J Appl Meteor 40(10):1762–1768, DOI 10.1175/1520-0450(2001)040<1762:FASOCM>2.0.CO;2

Poggi D, Katul GG (2007) Turbulent flows on forested hilly terrain: the recirculation region. Quart J Roy Meteorol Soc 133:1027–1039, DOI 10.1002/qj.73

Ross AN (2008) Large eddy simulations of flow over forested ridges. Boundary-Layer Meteorol 128:59–76, DOI 10.1007/s10546-008-9278-x

Ross AN (2011) Scalar transport over forested hills. Boundary-Layer Meteorol 141:179–199, DOI 10.1007/s10546-011-9628-y

Ross AN (2012) Boundary-layer flow within and above a forest canopy of variable density. Quart J Roy Meteorol Soc 138:1259–1272, DOI 10.1002/qj.989

Ross AN, Baker TP (2013) Flow over partially forested ridges. Boundary-Layer Meteorol 146:375–392, DOI 10.1007/s10546-012-9766-x

Ross AN, Grant ER (2015) A new continuous planar fit method for calculating fluxes in complex, forested terrain. Atmos Sci Lett 16:445–452, DOI 10.1002/asl.580

Ross AN, Harman IN (2015) The impact of source distribution on scalar transport over forested hills. Boundary-Layer Meteorol 156:211–230, DOI 10.1007/s10546-015-0029-5

Ross AN, Vosper SB (2005) Neutral turbulent flow over forested hills. Quart J Roy Meteorol Soc 131:1841–1862, DOI 10.1256/qj.04.129

Ross AN, Arnold S, Vosper SB, Mobbs SD, Dixon N, Robins AG (2004) A comparison of wind tunnel experiments and numerical simulations of neutral and stratified flow over a hill. Boundary-Layer Meteorol 113(3):427–459, DOI 10.1007/s10546-004-0490-z

Schlegel F, Stiller J, Bienert A, Maas HG, Queck R, Bernhofer C (2015) Large-eddy simulation study of the effects on flow of a heterogeneous forest at sub-tree resolution. BLM 154:27–56, DOI 10.1007/s10546-014-9962-y

Wilson JD, Finnigan JJ, Raupach MR (1998) A first-order closure for disturbed plant-canopy flows, and its application to winds in a canopy on a ridge. Quart J Roy Meteorol Soc 124:705–732, DOI 10.1002/qj.49712454704

Wood N (1995) The onset of separation in neutral, turbulent flow over hills. Boundary-Layer Meteorol 76:137–164, DOI 10.1007/BF00710894

Wood N, Mason PJ (1993) The pressure force induced by neutral, turbulent flow over hills. Quart J Roy Meteorol Soc 119:1233–1267, DOI 10.1002/qj.49711951402

Yang B, Raupach MR, Shaw RH, Tha K, Paw U KT, Morse AP (2006) Large-eddy simulation of turbulent flow across a forest edge. Part 1: Flow statistics. Boundary-Layer Meteorol 120(3):377–412, DOI 10.1007/s10546-006-9057-5